Nonlinear Dynamics and Systems Theory, **23** (2) (2023) 214–226

A New Hidden Attractor Hyperchaotic System and Its Circuit Implementation, Adaptive Synchronization and FPGA Implementation

R. Rameshbabu *, K. Kavitha, P. S. Gomathi and K. Kalaichelvi

Department of Electronics and Communication Engineering, V.S.B. Engineering College, Tamilnadu, Karur, India

Received: November 17, 2022; Revised: April 4, 2023

Abstract: In this paper, a new hyperchaotic system with no rest point is presented and its basic properties such as divergence and convergence, rest points and instability, Lypunov exponents, and bifurcation are analyzed in detail. In the proposed system, some special features such as position controllability and multistability in periodic state are observed. The analog circuit realization of the proposed hyperchaotic system is also presented to validate the present theoretical study of the system. Furthermore, the adaptive synchronization of the proposed hyperchaotic system is demonstrated using a novel anti-synchronization methodology. This paper also presents the Field Programmable Gate Array based digital circuit realization of adaptive anti-synchronization methodology for the proposed hyperchaotic system. The digital circuit implementation is achieved by generating the VHDL code for the FPGA implementation in Matlab and Xilinx. The experimental results are provided to verify the feasibility and effectiveness of our proposed scheme.

Keywords: *hidden attractor; hyperchaotic system; circuit implementation; adaptive synchronization; FPGA implementation.*

Mathematics Subject Classification (2010): 93-XX.

* Corresponding author: mailto:ramarrameshbabu@gmail.com

1 Introduction

The hyperchaotic system is a nonlinear dynamical system with at least two positive Lyapunov exponents. The positive Lyapunov exponents indicate the complexity and unpredictable response of a dynamical system. Due to this complex nature, the hyperchaotic system is used in many engineering fields such as oscillators [1], image encryption [2] and secure communication [3] etc. Recently, many hyperchaotic systems with hidden attractors have been introduced [4–6] and their dynamic behaviors are discussed in detail.

In this paper, another hyperchaotic system with hidden attractor is proposed and its basic dynamic properties and bifurcation are studied in detail. The proposed system also exhibits some special features such as multistability and offset boosting property for various applications. Multistability is an important phenomenon by which the chaotic system generates various number of attractors for different initial conditions. The multistability feature is observed in a periodic state in the proposed system. The position of the proposed attractor is controllable by introducing a controller in one of the state variable and this is known as the offset boosting control. The proposed system has three nonlinear terms. It is exciting to observe that our proposed system has no rest point and hence, its attractor is masked. In order to verify the dynamical behavior of our proposed system, the electronic circuit realization is presented in this paper. The circuit realization is based on discrete components and Integrated Circuits (IC) and simulated using MULTISIM software.

The trajectory of a hyperchaotic signal highly depends on its initial points and the parameters of the system are uncertain in practice. Therefore, there is a need to design a controller function to synchronize the even identical hyperchaotic systems with unknown parameters. Recently, many chaos synchronization methodologies have been proposed in literature reviews [7–9]. In this research paper, an anti-synchronization scheme is chosen for the demonstration of adaptive synchronization of the proposed system.

The digital realization of an adaptive synchronization scheme for chaotic systems has predominant applications in many digital chaotic systems such as digital data transmission [10] etc. In order to expand the hyperchaos based real time applications, nowadays, researchers give more attention to the implementation of a hyperchaotic system in digital circuits such as Field Programmable Gate Array (FPGA) [11], [12]. Based on the literature survey, in this work, the proposed adaptive anti-synchronization scheme for the hyperchaotic system is realized in FPGA using MATLAB simulink and Xilinx system generator tools.

2 Modelling of New Hidden Attractor Hyperchaotic System

The new hyperchaotic system with hidden attractor is of the form

$$\begin{aligned} \dot{p} &= \alpha(q-p), \\ \dot{q} &= \beta q - pr + w, \\ \dot{r} &= pq - \gamma r, \\ \dot{w} &= w - pr. \end{aligned} \tag{1}$$

Here, p, q, r, w are the state variables and α, β, γ are the non zero positive parameters of the system (1). The system parameter values are chosen as $\alpha = 26$, $\beta = 14$ and $\gamma = 3$. The behavior of the new dynamical system (1) never changes the polarity of the co-ordinates changes as $(p, q, r, w) \to (-p, -q, r, -w)$ and the proposed system has rotational symmetry about the r-axis. The divergence of the system (1) is given as $\nabla f = \frac{\partial f_p}{\partial p} + \frac{\partial f_q}{\partial q} + \frac{\partial f_r}{\partial r} + \frac{\partial f_w}{\partial w} = -14.36$, where $f_p = \dot{p}$, $f_q = \dot{q}$, $f_r = \dot{r}$, $f_w = \dot{w}$. Since the divergence of (1) is negative for all positive values of α,β,γ, we can conclude that the proposed system has a strange attractor. The rest points of the proposed system (1) can be computed numerically by equating the Equation (1) to zero as given in Equation (2),

$$
\begin{aligned}
\alpha(q-p) &= 0, \\
\beta q - pr + w &= 0, \\
pq - \gamma r &= 0, \\
w - pr &= 0.
\end{aligned}
\tag{2}
$$

From Equation (2), the rest points of system (1) are computed as $E\{0,0,0,0\}$ and it is observed that the attractor of new dynamical system (1) is masked up somewhere in phase space. The Jacobian matrix of the system (1) is given as

$$
J = \begin{pmatrix} -\alpha & \alpha & 0 & 0 \\ -r & \beta & -p & 1 \\ q & p & -\gamma & 0 \\ -r & 0 & -p & 1 \end{pmatrix}.
\tag{3}
$$

The eigenvalues of the Jacobian matrix (J) can be obtained as $\lambda_1 = -26, \lambda_2 = 14, \lambda_3 = -3$ and $\lambda_4 = 1$. Since the set of eigenvalues has both positive and negative real values, the rest point E is an unstable point. The Lyapunov exponents of the new hyperchaotic dynamic system (1) are calculated using the Wolf algorithm as $LE = [0.331891, 0.038063, 0, -14.314174]$ for the initial conditions $p_0 = 1, q_0 = 2, r_0 = 1, w_0 = 3$. The sum of Lyapunov exponents is $-13.94422 < 0$ and hence, the proposed system (1) is dissipative. The Lyapunov dimension (D_L) can be obtained as $D_L = 3 + \frac{LE_1+LE_2+LE_3}{|LE_4|} = 3.019644$, which indicates the fractional dimension of the proposed system (1).

3 Dynamic Analysis of Proposed System

The variations of state variables of the proposed hyperchaotic system (1) in 2D and 3D planes are given in Figure 1. The bifurcation diagrams and Lyapunov exponents of the proposed system (1), based on the parameters α and β for the initial conditions {0, 1, -1, 1}, are shown in Figure 2. First, the parameter α varies in the range of $\alpha\epsilon[22-27]$ and the remaining parameters are kept constant, as demonstrated in Figure 2a, which shows that the system (1) is in a period state in the range of $\alpha\epsilon[22-22.3]$, $\alpha\epsilon[24.3-25.5]$ and in chaos states in the range of $\alpha\epsilon[22.3-24.2]$, $\alpha\epsilon[25.5-27]$. Second, the parameter β varies in the range of $\beta\epsilon[13-18]$ and the other parameters are kept constant as given in Figure 2b, which shows that there is the inverse doubling behavior. It is in a chaotic state in the range of $\beta\epsilon[13-14.5]$, and in a period state in the range of nearly $\beta\epsilon[14.5-15.4]$ and $\beta\epsilon[17.5-18]$. The Lyapunov spectrum versus the various parameters is also demonstrated in Figures 2c and 2d, in which LE_1, LE_2, LE_3 and LE_4 are represented in blue, red, green, and cyan, respectively.

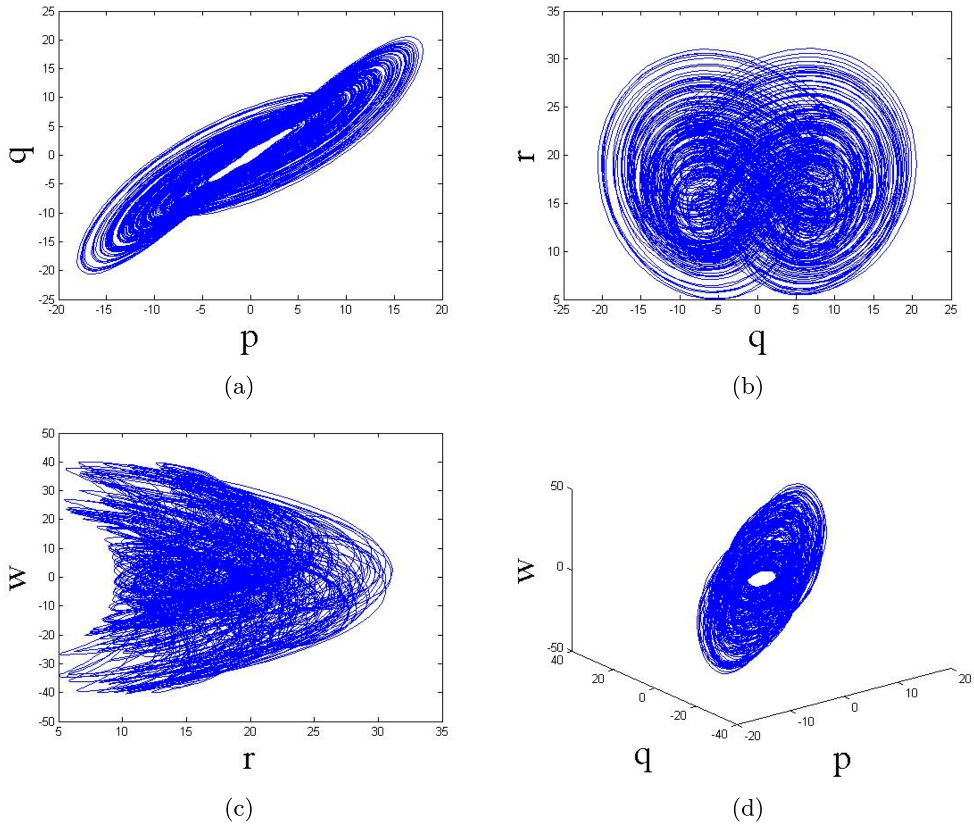

Figure 1: Attractors of the proposed hyperchaotic system.

4 Controllability of Proposed Hyperchaotic System

The position of the proposed attractor is controllable by introducing a controller parameter δ in the state variable w in the proposed system (1). The state variable w in the proposed system is replaced with $w + \delta$ as given in (4). Figure 3a shows the position of the proposed controlled attractor in the $r - w$ plane for $\delta = 0$ (blue), $\delta = -90$ (black) and $\delta = 90$ (magenta). Figure 3b shows that the state variable w is converted from bipolar into unipolar by varying the controller value.

$$\begin{aligned}
\dot{p} &= \alpha(q - p),\\
\dot{q} &= \beta q - pr + (w + \delta),\\
\dot{r} &= pq - \gamma r,\\
\dot{w} &= (w + \delta) - pr.
\end{aligned} \tag{4}$$

5 Multistability of Proposed Hyperchaotic System

Multistability or a multiple attractor property is observed in the various periodic states of the proposed system. Figure 4a shows a bifurcation diagram for the parameter β

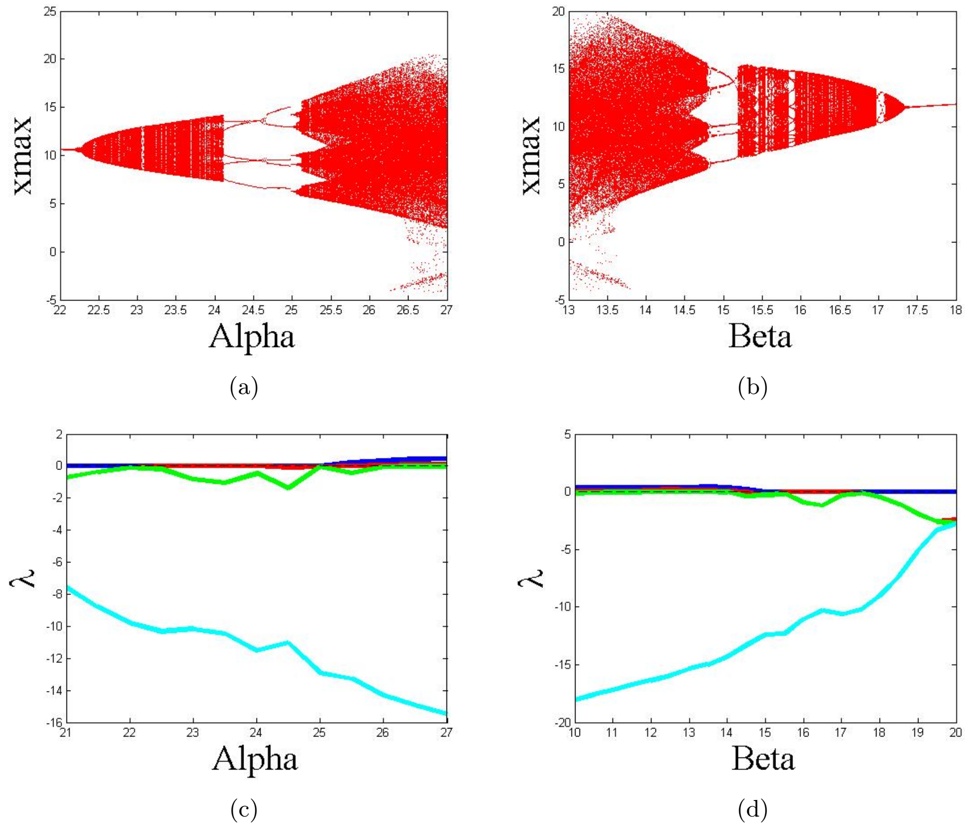

Figure 2: (a-b) Bifurcation diagram, (c-d) Lyapunov exponents plots of the proposed system.

under the initial conditions $(0, 1, -1, 1)$ (red) and $(1, 1, -1, 1)$(black) and indicates that there is a multiple attractor in periodic states. Figure 4b shows the phase portraits of the proposed system when $a = 26, b = 15, c = 3$ under the initial conditions $(0, 1, -1, 1)$ (blue) and $(1, 1, -1, 1)$ (magenta).

6 Electronic Circuit Implementation of Proposed Hyperchaotic System

In this section, an analog circuit is constructed to confirm the theoretical results of the proposed system (1) using electronic components such as resistors, capacitors, OPAMP 741, and multiplier. The time and amplitude scaling factors are chosen as $T = 100t$ and $A = 5$, respectively, to realize the circuit parameters α, β and γ. The system (1) can be written as (5),

$$\begin{aligned} \tfrac{dx}{dT} &= 100\alpha(y - x), \\ \tfrac{dy}{dT} &= 100(\beta y - Axz + w), \\ \tfrac{dz}{dT} &= 100(Axy - \gamma z), \\ \tfrac{dw}{dT} &= 100(w - Axz). \end{aligned} \tag{5}$$

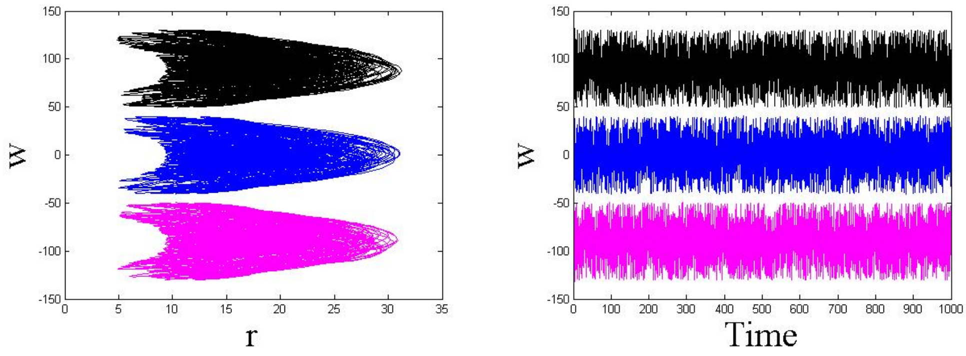

(a) (b)

Figure 3: Position variation of the proposed attractor with $\delta = 0$(Blue), $\delta = 90$(Magenta), $\delta = -90$(Black). (a) $r - w$ plane, (b) The time series of the state variable w.

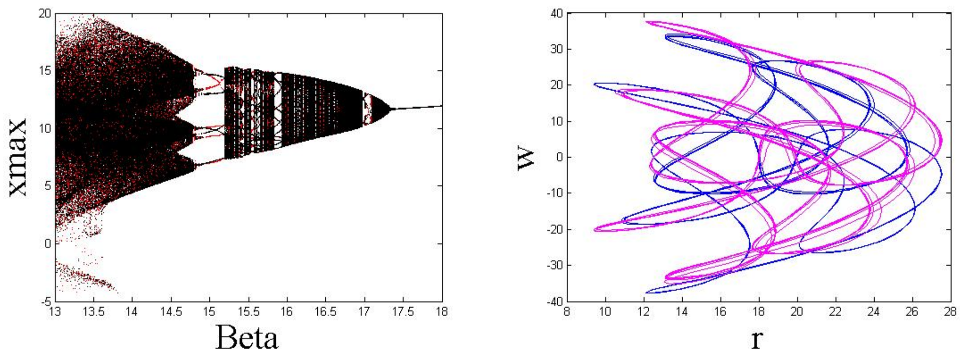

(a) Bifurcation diagram for β (b) $\alpha = 26, \beta = 15, \gamma = 3$

Figure 4: Multistability behaviour of the proposed system.

The equations for the proposed electronic circuit design can be given as in Equation (6),

$$\begin{aligned}
\frac{dx}{dT} &= \frac{R_1}{R_2R_3C_1}(-y) - \frac{R_1}{R_2R_4C_1}(x),\\
\frac{dy}{dT} &= \frac{R_5}{R_6R_7C_2}(-y) - \frac{R_5}{10R_6R_9C_2}(xz) - \frac{R_5}{R_6R_8C_2}(-w),\\
\frac{dz}{dT} &= \frac{R_{10}}{R_{11}R_{12}C_3}(-xy) - \frac{R_{10}}{R_{11}R_{13}C_3}(z),\\
\frac{dw}{dT} &= \frac{R_{14}}{R_{15}R_{16}C_4}(-w) - \frac{R_{14}}{R_{15}R_{17}C_4}(-xz).
\end{aligned} \tag{6}$$

The circuit realization of system (6) using Multisim software is shown in Figure 5. The electronic components are chosen as $C_1 = C_2 = C_3 = C_4 = 10$nF, $R_1 = R_5 = R_{10} = R_{14} = R_{18} = R_{19} = R_{20} = R_{21} = R_{22} = R_{23} = R_{24} = R_{25} = 100\Omega$, $R_2 = R_6 = R_{11} = R_{15} = 50k\Omega$, $R_3 = R_4 = 77k\Omega$,$R_7 = 143k\Omega$, $R_8 = R_{16} = 2000k\Omega$,$R_9 = R_{12} = R_{17} = 40k\Omega$ and $R_{13} = 595k\Omega$. Circuit simulation results are shown in Figure 6. Note that the Multisim simulation results are agreeing with the Matlab results shown in Figure 1.

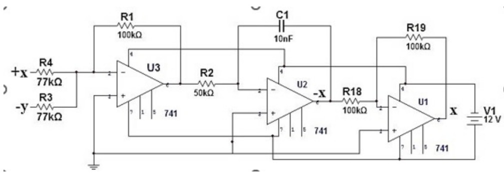

(a) x signal

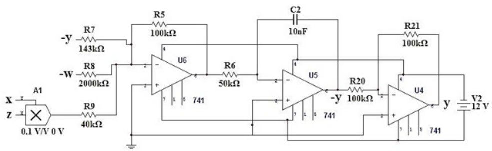

(b) y signal

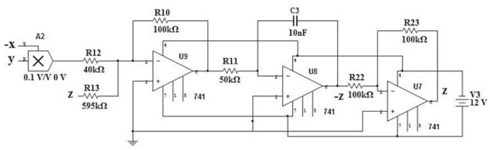

(c) z signal

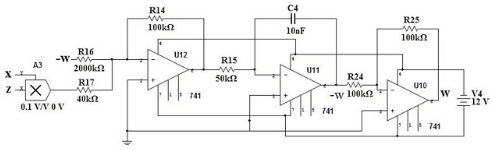

(d) w signal

Figure 5: Circuit realization of the proposed system.

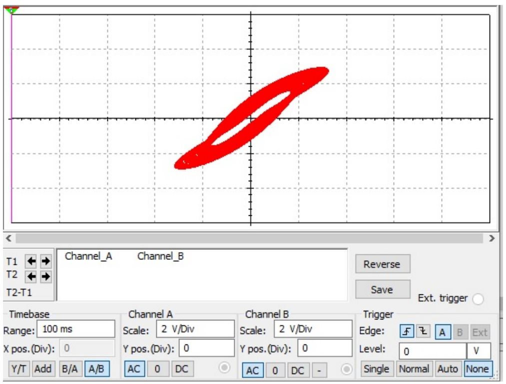

(a) xy

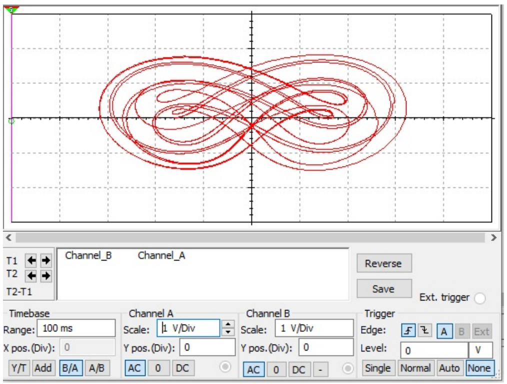

(b) yz

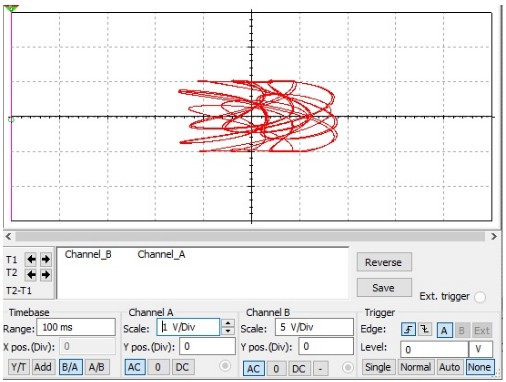

(c) zw

Figure 6: Electronic simulation result for the proposed system.

7 Adaptive Synchronization of Proposed Hyperchaotic System

In this section, the anti-synchronization of the proposed system (1) is established using an adaptive control method. In the last two decades, a variety of synchronization schemes such as fuzzy set based methods [13], observer-based methods [14], Lyapunov-based methods [15], sliding surface-based methods [16], PID control [17], and active method [18] were used. However, the synchronization schemes proposed in the literature review [13–18] have some limitations. The fuzzy set methods need the states of the system for the calculations of membership and non - membership functions and building a regressor vector. The observer-based synchronization scheme is restricted to synchronize different systems since the structure of the slave system is defined by the master system. In backstepping, synchronization is a Lyapunov-based synchronization method in which the calculation of the Lyapunov exponent is required for the entire system. The sliding mode control method requires the design of a sliding surface in which the states of the system sliding on the sliding surface and the dynamic behavior of the system depend on the sliding surface equations. The chattering problem is the main drawback of the sliding mode controller. The Proportional Integral Derivative (PID) controller has low robustness and suitability for linear systems. The active control method is not suitable for practical situations since the initial conditions and the system parameters are unknown in practice. The literature review on chaos synchronization pinpoints that compared to any other method, the adaptive feedback control method is a simple, convenient, and efficient methodology for implementing the chaos synchronization. The master and the slave system are given as in (1) and (7), respectively,

$$
\begin{aligned}
\dot{p_1} &= \alpha(q_1 - p_1) + u_1,\\
\dot{q_1} &= \beta q_1 - p_1 r_1 + w_1 + u_2,\\
\dot{r_1} &= p_1 q_1 - \gamma r_1 + u_3,\\
\dot{w_1} &= w_1 - p_1 r_1 + u_4.
\end{aligned}
\tag{7}
$$

Here, p_1, q_1, r_1 and w_1 are the state variables of the slave system, u_1, u_2, u_3 and u_4 are the adaptive controllers used to synchronize the master and the slave system, $\alpha = 26, \beta = 14, \gamma = 3$ are the system parameters. The anti-synchronization error between the master and the slave system can be written as (8),

$$
\begin{aligned}
e_1 &= p_1 + p,\\
e_2 &= q_1 + q,\\
e_3 &= r_1 + r,\\
e_4 &= w_1 + w.
\end{aligned}
\tag{8}
$$

Based on adaptive control theory, the adaptive controllers can be derived as (9),

$$
\begin{aligned}
\dot{u_1} &= -\hat{\alpha}(e_2 - e_1) - g_1 e_1,\\
\dot{u_2} &= -\hat{\beta} e_2 + e_4 + p_1 r_1 + pr - g_2 e_2,\\
\dot{u_3} &= \hat{\gamma} e_3 - p_1 q_1 - pq - g_3 e_3,\\
\dot{u_4} &= -e_4 + p_1 r_1 + pr - g_4 e_4.
\end{aligned}
\tag{9}
$$

Here, $\hat{\alpha}, \hat{\beta}, \hat{\gamma}$ are the estimate values of the unknown parameters α, β, γ, respectively. g_1, g_2, g_3, g_4 are the gain of the controllers. Consider a Lyapunov function candidate as

$$
\begin{aligned}
V &= e_1\dot{e}_1 + e_2\dot{e}_2 + e_3\dot{e}_3 + e_4\dot{e}_4 + e_a\dot{e}_a + e_b\dot{e}_b + e_c\dot{e}_c\\
&= e_a[e_1(e_2 - e_1) - \dot{\hat{\alpha}}] + e_b[e_2^2 - \dot{\hat{\beta}}] + e_c[-e_3^2 - \dot{\hat{\gamma}}] - g_1 e_1^2 - g_2 e_2^2 - g_3 e_3^2 - g_4 e_4^2.
\end{aligned}
\tag{10}
$$

By choosing the dynamics of unknown parameter values as $\dot{\hat{\alpha}} = e_1(e_2 - e_1)$, $\dot{\hat{\beta}} = e_2^2$ and $\dot{\hat{\gamma}} = -e_3^2$, Equation (10) becomes Equation (11) which indicates the negative Lyapunov function, the anti-synchronization error signals and the parameter error signals exponentially reach zero, which means that both the master and the slave system are synchronized together.

$$V = -(g_1 e_1^2 + g_2 e_2^2 + g_3 e_3^2 + g_4 e_4^2) < 0. \tag{11}$$

To demonstrate the adaptive synchronization of the proposed system, different initial conditions are chosen for the master and the slave system separately such as $X_m = (3, -7, 1.5, 6)$ and $X_s = (2, 3, 4, 1)$. The initial conditions for the positive parameters α, β, γ are, respectively, taken for demonstration as (0.5,0.2,0.7). The gain of the adaptive controllers is also chosen for the demonstration purpose as $g_i = 1$, where $i = 1, 2, 3, 4$. Figure 7a shows that the anti$-$synchronization errors e_1, e_2, e_3 and e_4 become zero when both the master and the slave system are synchronized together. Figure 7b represents the synchronized state variables for the simulation time $1500s$. The dotted line represents the master system and the solid line represents the controlled slave system $p - p_1$ (Blue), $q - q_1$ (Brown), $r - r_1$ (Magenta) and $w - w_1$ (Red).

8 FPGA Implementation of Adaptive Synchronization of Proposed Hyperchaotic System

In this section, an FPGA-based digital circuit realization of the proposed adaptive synchronization methodology for a new hyperchaotic system is presented. The digital realization of the synchronized hyperchaotic system is achieved in the MATLAB and Xilinx environments. In this methodology, initially, Equations (1) and (7) to (9) are constructed in MATLB simulink using Xilinx system generator tools to generate the VHDL code. Then, the generated VHDL code is simulated and synthesized in Xilinx software. Figure 8 shows the digital circuit realization of the proposed hyperchaotic system. The initial conditions for the master and the slave system are chosen for the FPGA implementation of the synchronization methodology as $(p(0), q(0), r(0), w(0)) = (5, 2, 3, 1)$ and $(p_1(0), q_1(0), r_1(0), w_1(0)) = (20, 30, 25, 15)$, respectively. Hence, the initial conditions for the anti-synchronization error signal can be from Equation (8): $(e_1(0), e_2(0), e_3(0), e_4(0)) = (25, 32, 28, 16)$. The model of the proposed anti-synchronization methodology is shown in Figure 9, which shows the coupling between Equations (1) and (7) to (9). In Figure 9, p_0 and q_0 are the initial conditions for the master and the slave system, $p_i\, outnet\, [31:0]$ is the 32-bit state signal of the master system and $q_i\, outnet\, [31:0]$ is the 32-bit state signal of the slave system. α_0, β_0, and γ_0 are the initial conditions for the parameters α, β, and γ, respectively. The master block is shown in Figure 8, the controller block contains Equation (10), parameter and error signal block generate the anti-synchronization error signals, and the initial conditions are fed in the master and slave system block. The VHDL code for the proposed synchronization methodology is generated for the FPGA device virtex-xc6vsx315t3ff1156. After that, the generated code is simulated in Xilinx software using ISE simulator.

As a result of simulation, a small portion of discrete waveform for the proposed anti-synchronization methodology is obtained as given in Figure 11, in which the signals $x_1 outnet[31:0]$ to $x_4\, outnet\, [31:0]$ represent the signals from the master system, the signals $y_1\, outnet\, [31:0]$ to $y_4\, outnet\, [31:0]$ represent the signals from the slave system, and $e_1\, outnet\, [31:0]$ to $e_4\, outnet\, [31:0]$ are the error signals. For instance,

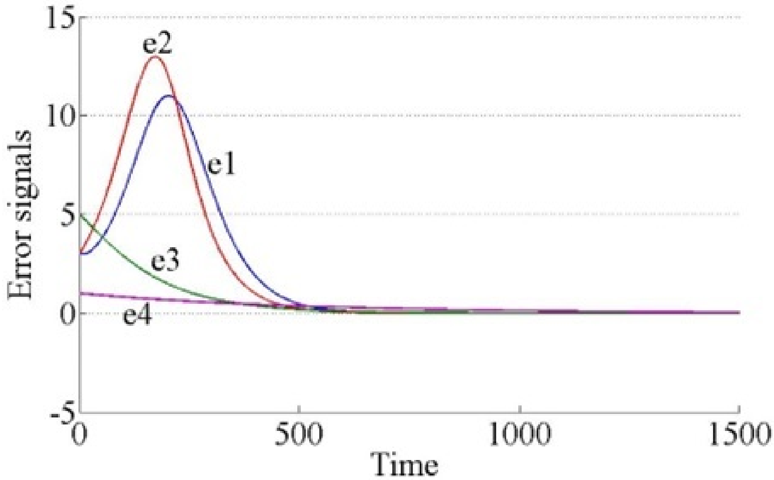

(a) Time variation of error signals.

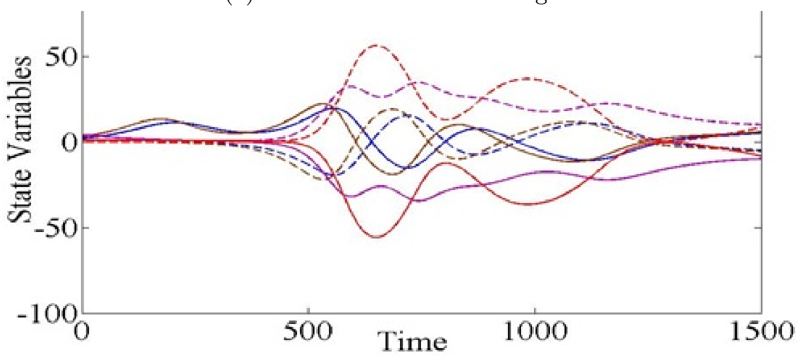

(b) Synchronized master and slave system.

Figure 7: Simulation result for the adaptive synchronization of the proposed system.

x_1 *outnet* [31 : 0] has the value 0000000000000101, which is equivalent to $x_1(0) = 5$, and y_1 *outnet* [31 : 0] has the value 0000000000010100, which is equivalent to $y_1(0) = 20$, and the anti-synchronization error e_1 *outnet* [31 : 0] has the value 0000000000011001, which is equivalent to $e_1(0) = 25$. Thus, we can conclude that the VHDL code simulation result agrees with the theoretical model developed for the adaptive anti-synchronization methodology in Section 7.

The resource utilization for virtex-xc6vsx315t3ff1156 is given in Table 1, which shows that the proposed synchronization methodology utilizes a very small amount of the available source.

9 Conclusion

A new hyperchaotic system with no rest point or hidden attractors is investigated, and numerical and analytical studies are carried out on its basic properties. The new system has two positive, 4-dimensional Lyapunov exponents, no rest points, and is unstable,

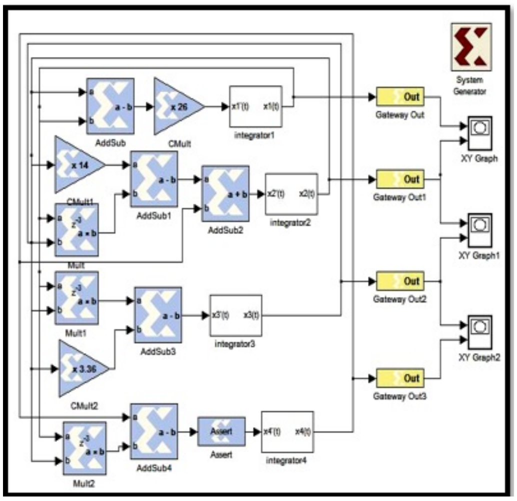

Figure 8: Digital realization of the proposed hyperchaotic system.

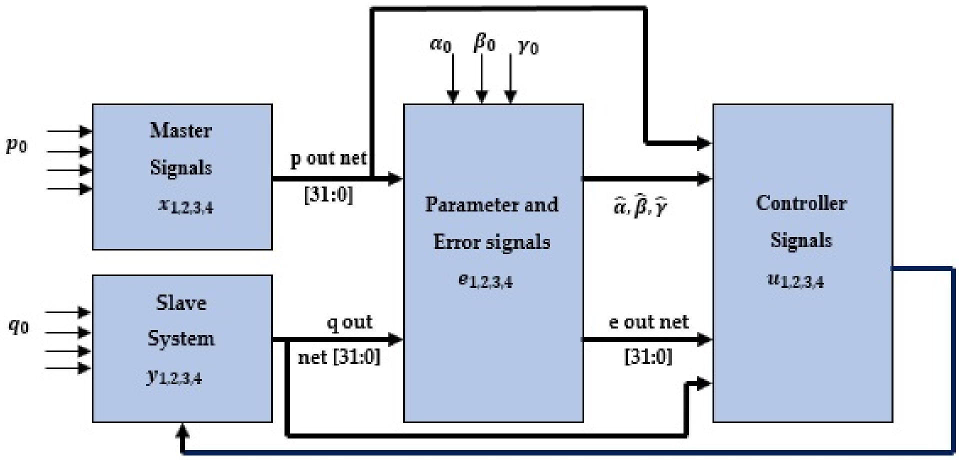

Figure 9: Coupling between the master and the slave hyperchaotic system.

which means that the proposed system has a hyperchaotic nature. The dynamical analysis of the proposed system is conducted using a bifurcation diagram and a Lyapunov exponents spectrum. An analog circuit for the new hyperchaotic system is constructed and simulated in Multisim and the simulation results show the viability of the proposed theoretical modeling of the new system. By using the adaptive control methodology, the anti-synchronization of a new, identical hyperchaotic system is studied. The Matlab simulation results for the adaptive anti-synchronization are demonstrated with different initial conditions to verify the theoretical analysis of the designed controllers. In order to digitize the synchronization methodology, FPGA implementation of the new synchronized hyperchaotic system with hidden attractors is designed. The simulation results and FPGA outputs demonstrate the efficiency of the proposed digitization methodology

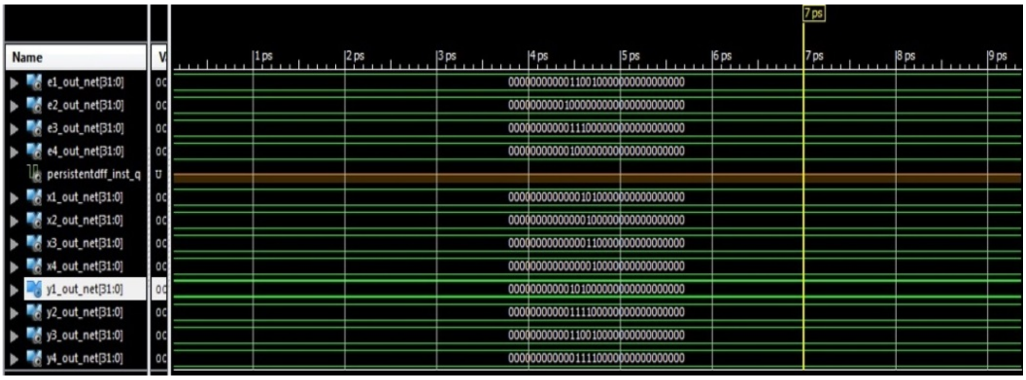

Figure 10: Simulation result of VHDL code for the proposed anti - synchronized hyperchaotic system.

	Used Sources	Available Sources	Percentage
Number of Slice Registers	2502	393,600	1
Number of Slice LUTs	4775	196,800	2
Number of Occupied Slices	1466	49,200	2
Number of Bonded IOBs	193	600	32
Number of BUFG/BUFGCTRLs	1	32	0.3

Table 1: Utilization of resources for virtex-xc6vsx315t3ff1156.

for the adaptive anti-synchronization scheme for a new hyperchaotic system with hidden attractors.

References

[1] T. Fonzin Fozin, P. Megavarna Ezhilarasu, Z. Njitacke Tabekoueng, G. D. Leutcho, J. Kengne, K. Thamilmaran, A. B. Mezatio and F. B. Pelab. On the dynamics of a simplified canonical Chua's oscillator with smooth hyperbolic sine nonlinearity: Hyperchaos, multistability and multistability control. *Chaos Interdisciplinary Journal of Nonlinear Science* **29** (2019) 11315.

[2] A. Arab, M.J̇. Rostami and B. Ghavami. An image encryption method based on chaos system and AES algorithm. *Journal of Super computing* **75** (2019) 6663–6682.

[3] J. P. Singh, K. Lochan and B. K. Roy. Secure communication using new hyperchaotic system with hidden attractors. In: *Lecture Notes in Electrical Engineering* (Eds.: C. Shreesha and R. Gudi). Springer, Singapore, 2020, 67–69.

[4] A. Al-khedhairi, A. Elsonbaty, A. H. Abdel kader, and A. A. Elsadany. Dynamic analysis and circuit implementation of new 4D Lorenz type hyperchaotic system. *Mathematical Problems* **2019** (2019) 6581586.

[5] X. Zhang and C. Wang. Multi scroll hyperchaotic system with hidden attractors and its circuit implementation. *International Journal of Bifurcation and Chaos* **29** (2019) 1950117.

[6] L. G. Dolvis, S. Vaidhyanathan, K. Jacques,A. Sambas and M. Mamat. A new 4 D hyperchaotic system with four scroll hidden attractor, its properties and bifurcation analysis. *International Journal of Bifurcation and Chaos* **29** (2019) 1950117.

[7] S. Sajjadi, D. Baleanu, A. Jajarmi and H. M. Pirouz. A new adaptive synchronization and hyperchaos control of a biological snap oscillator. *Chaos, Solitons and Fractals* **138** (2020) 109919.

[8] A. Jajarmi, M. Hajipour and D. Baleanu. New aspects of the adaptive synchronization and hyperchaos suppression of a financial model. *Chaos, Solitons and Fractals* **99** (2017) 285–296.

[9] T. Khan and H. Chaudhary. Adaptive controllability of microscopic chaos generated in chemical reactor system using anti-synchronization strategy. *Number Algebra, Control and Optimization* **12** (2021) 611–620.

[10] G. Kaddoum. Wireless Chaos-Based Communication Systems: A Comprehensive Survey. *IEEE Access* **4** (2016) 2621-2648.

[11] R. Rameshbabu, and G. R. Suresh. Design of adaptive feedback control for new 3D chaotic system and its digital implementation on FPGA. *Indian Journal of Science and Technology* **13** (2020) 1977-1990.

[12] R. Karthikeyan, A. Prasina, R. Babu, and S. Raghavendran. FPGA implementation of novel synchronization methodology for new chaotic system. *Indian Journal of Science and Technology* **8** (2015) 47901.

[13] S. Helmy, M. Magdy, and M. Hamdy. Control in the loop for synchronization of nonlinear chaotic systems via adaptive intuitionistic neuro-fuzzy: A comparative study. *Complex and Intelligent Systems* **8** (2022) 3437–3450.

[14] S. Kaouache, N. E. Hamri, A. S. Hecinliyan, E. Kandiran, B. Druni and A. C. Keles. Increased Order Generalized Combination Synchronization of Non-Identical Dimensional Fractional-Order Systems by Introducing Different Observable Variable Functions. *Nonlinear Dynamics and System Theory* **20** (2020) (3) 307–315.

[15] M. K. Shukla, and B. B. Sharma. Backstepping based stabilization and synchronization of a class of fractional order chaotic systems. *Chaos, Solitons and Fractals* **102** (2022) 274–284.

[16] L. M. Wang. Model-free adaptive sliding mode controller design for generalized projective synchronization of the fractional-order chaotic system via radial basis function neural networks. *Pramana Journal of Physics* **89** (2017) 38.

[17] M. M. Zirkohi. Chaos synchronization using higher-order adaptive PID controller. *AEU International Journal of Electronics and Communication* **94** (2018) 157–167.

[18] M. Labid, and N. Hamri. A Chaos Synchronization between Fractional-Order Lesser Date Moth Chaotic System and Integer-Order Chaotic System via Active Control. *Nonlinear Dynamics and System Theory* **22** (4) (2022) 407–413.